Science in China Series G: Physics, Mechanics & Astronomy

www.scichina.com
phys.scichina.com
www.springerlink.com

Giant enhancement of magnetocaloric effect in metallic glass matrix composite

WANG YongTian, BAI HaiYang, PAN MingXiang, ZHAO DeQian & WANG WeiHua†

Institute of Physics, Chinese Academy of Sciences, Beijing 100080, China

The magnetocaloric effect (MCE) has made great success in very low temperature refrigeration, which is highly desirable for application to the extended higher temperature range. Here we report the giant enhancement of MCE in the metallic glass composite. The large magnetic refrigerant capacity (*RC*) up to 10^3 J·kg^{-1} is more than double the *RC* of the well-known crystalline magnetic refrigerant compound $Gd_5Si_2Ge_{1.9}Fe_{0.1}$ (357 J·kg^{-1}) and $MnFeP_{0.45}As_{0.55}$ (390 J·kg^{-1})(containing either exorbitant-cost Ge or poisonous As). The full width at half maximum of the magnetic entropy change (ΔS_m) peak almost spreads over the whole low-temperature range (from 303 to 30 K), which is five times wider than that of the $Gd_5Si_2Ge_{1.9}Fe_{0.1}$ and pure Gd. The maximum ΔS_m approaches a nearly constant value in a wide temperature span over 100 K, and however, such a broad table-like region near room temperature has seldom been found in alloys and compounds. In combination with the intrinsic amorphous nature, the metallic glass composite may be potential for the ideal Ericsson-cycle magnetic refrigeration over a broad temperature range near room temperature.

metallic glass, magnetocaloric effect, composite

1 Introduction

The magnetocaloric effect (MCE) is a temperature change of a material that occurs when a magnetic field is applied under adiabatic conditions, which has been restricted to very low temperature cryogenic applications for decades[1−4]. Recently, large numbers of MCE materials with a higher magnetic transition temperature (such as room temperature) have attracted much attention for refrigeration as an environment-friendly and high-efficiency alternative to conventional vapour-cycle refrigerants[2,3]. Above 15 K, since the thermal agitation energy and the lattice entropy increase considerably, an Ericsson-cycle based magnetic refrigerator can utilize heat as much as possible, due to the fact that the magnetic entropy change ΔS_m of an active magnetic regenerator

Received December 24, 2007; accepted February 1, 2008
doi: 10.1007/s11433-008-0053-2
†Corresponding author (email: whw@aphy.iphy.ac.cn)
Supported by the National Natural Science Foundation of China (Grant Nos. 50621061 and 50731008) and the National Basic Research Program of China (973 Program) (Grant No. 2007CB613904)

material is independent of the change of lattice contribution to the material's total entropy[5−7]. For optimum efficiency and feasibility, the ideal magnetic refrigerant suitable for working in a broad temperature range between 15 K and room temperature should be an Ericsson-type refrigerator with a constant ΔS_m over a wide temperature span (so called table-like)[5−8]. However, this feature has seldom been found in alloys or compound materials (e.g. GdSiGe[2,4], MnFePAs[3]), which generally possess a sharp magnetic change peak at Curie temperature and fall off rapidly on both sides.

In an attempt to circumvent this problem, multiplayers or physical mixed composites have been developed[6,9,10], where the ferromagnetic materials with varying Curie temperature are layered, pressed or sintered to span the full temperature range of the thermodynamic cycle. While other serious problems in these systems, including solid-state reactions between constituent materials and entropy generation in physical mixtures due to temperature differences between neighboring particles, alter the expected temperature profile of ΔS_m and reduce the overall efficiency of the thermodynamic cycle[5,7]. Therefore, it is expected that the best choice for an ideal Ericsson-cycle refrigerant would be a single material with a temperature independent of the magnetic entropy change, which can make the construction of magnetic refrigerator much simpler. The typical materials with such properties are a series of (GdEr)NiAl crystalline alloys[5], in which the table-like temperature region is not smooth enough and confined in a low and narrow temperature span (from 20 to 50 K). Near room temperature, few materials have been reported to show a relatively broad table-like ΔS_m region so far. On the other hand, before magnetic refrigeration becomes a viable cooling technology, there are also other key issues that need to be settled. The applied magnetic field must be reduced below 20 kOe so as to allow the use of a low-cost permanent magnet instead of a superconducting magnet as the magnetic field source; the MCE material itself should be a highly effective recuperative heat exchanger working in conjunction with the pulsating heat transformer fluid[11], and there needs to be a layer structural refrigerant material with a high surface area to volume ratio, high shock resistance and corrosion resistance. Whereas many representative bulk crystal MCE materials such as Gd[12], GdAl[13] and GdSiGe[14] show the performance deterioration in the ribbon form as a result of the crystal structure changes during the melt-spinning process.

Very recently a series of heavy rare-earth (Gd, Dy, Er, Tb, Ho) based bulk metallic glasses have been developed[15−17]. The intrinsic glassy nature leads to low eddy current and hysteresis losses, tailorable composition, high corrosion resistance, large specific area and excellent mechanical properties[18−20], which opens up a possibility to enhance the MCE by the unique structural disorder. In this work, the repeatedly-stacked glassy ribbon is firstly verified to exhibit giant enhancement of low-field MCE over that in bulk glassy alloys. Then by virtue of the intrinsic phase separation and clustering in the metallic glasses, a FeGd-based stacked ribbon composite containing *in situ* formed nanocrystals is further developed. Thereby the greatly enhanced MCE makes the metallic glass composite ideal for the Ericsson-cycle magnetic refrigeration over the broad temperature range below room temperature.

2 Experimental

Master alloys were prepared by arc melting pure metals in a Ti-gettered argon atmosphere under ambient pressure, and the purity of the starting constituents was 99.9%. The ingots were ho-

mogenously remelted and suck-cast into a Cu mold under argon atmosphere to get the cylindrical rods of 1—2 mm in diameter. The ribbons were prepared by a single roller melt-spinning apparatus at wheel surface velocities of 5—80 m/s in argon atmosphere. The ribbons were cut into the pieces with the same length of 5 mm, and then these sheets were repeatedly stacked. The amorphous nature was characterized by X-ray diffraction (XRD) in a MAC M03 XHF diffractometer with Cu Kα radiation. Thermal analysis was performed using a Perkin-Elmer DSC-7 differential scanning calorimeter under a continuous argon flow at a heating rate of 20 K/min. The magnetism measurements were performed using a PPMS (physical property measurement system) 6000 of Quantum Design Company. The study of topography and domain structure was carried out by using Digital Instruments NanoScope IIIa D-3000 AFM/MFM.

3 Results

The magnetocaloric effect was determined by measuring the magnetization M as a function of the temperature T and the applied field H. The magnetic field with a maximal value of 50 kOe was used, the temperature step of 5 or 10 K was chosen in the regions far from T_c, and a step of 3 K was processed in the vicinity of T_c (smaller intervals provoke an increase in the noise due to the numerical derivatives of the curves). In an isothermal process of magnetization, the total magnetic entropy change of the system under a magnetic field can be derived from Maxwell relation by integrating over the magnetic field[2], $\Delta S_m = \int_{H_{min}}^{H_{max}} \left(\frac{\partial M}{\partial T}\right) dH$, where H_{min} (usually fixed to zero) and H_{max} represent the initial and final values of magnetic field, respectively. To derive the temperature dependence of magnetic entropy change, the numerical approximation of the integral is usually applied, $\Delta S_m = \sum_i \frac{M_i - M_{i+1}}{T_i - T_{i+1}} \Delta H$, where M_i and M_{i+1} are the experimental values of the magnetization at T_i and T_{i+1} under magnetic field H_i, respectively.

Figure 1(a) shows the two sets of isothermal magnetization curves M-H of a typical rare-earth-based metallic glass of $Gd_{53}Co_{20}Al_{24}Zr_3$ in bulk and repeatedly-stacked ribbon forms, respectively. They are measured in the same temperature range and step. ΔS_m under different magnetic fields shown in Figure 1(b) is determined by computing the area (i.e. the hatched region marked in Figure 1(a)) inside each magnetization M vs. H, and the solid line and dash line correspond to ΔS_{ribbon} and ΔS_{bulk}, respectively. For the same temperature interval, it can be seen clearly that the hatched area of the glass with stacked-ribbon is much larger than that in the bulk form, indicating the giant enhancement of ΔS_m, especially under low field. For other representative metallic glasses with different Curie temperatures, ΔS_m vs. T curves under 5 kOe are shown in Figure 1(c), and their ΔS_m peak values have been doubly enhanced in the stacked-ribbon structure compared with that in the bulk form. In addition, Figure 1(d) shows ΔS_m vs. T of the stacked ribbons containing three different rare-earth-based metallic glasses with a mass ratio of 1∶1∶1. Although nearly 50 at.% of the expensive Gd has been replaced by the low-cost metals of Co and Al, ΔS_m shows an approximate constant value between 10 and 100 K, which is about 50 percent larger than that of Gd_xDy_{1-x} crystal composite containing five constituents[10]. These indicate that the stacked-ribbon structure is a simple way to greatly enhance the low-field MCE of metallic glasses.

The full width at half maximum of the ΔS_m peak (ΔT_{FWHM}), shown in Figure 2(a), provides ad-

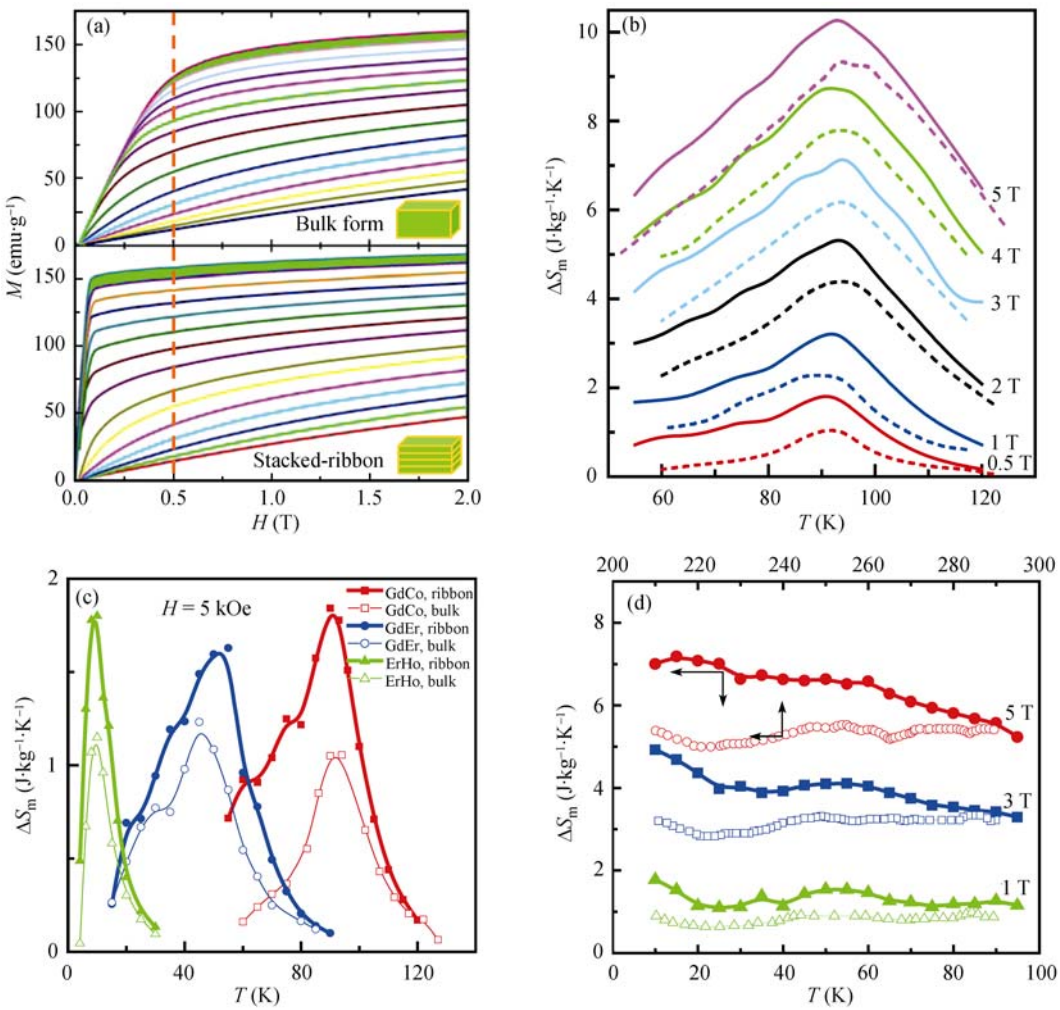

Figure 1 (a) The isothermal magnetization curves *M*-*H* of $Gd_{53}Co_{20}Al_{24}Zr_3$ metallic glass measured at different temperatures in bulk and stacked-ribbon forms, respectively. The insets show the schematic of the samples for the measurements. (b) The magnetic entropy change ΔS_m vs. T of $Gd_{53}Co_{20}Al_{24}Zr_3$ metallic glass under different magnetic fields. The solid line and dash line correspond to ΔS_{ribbon} and ΔS_{bulk}, respectively. (c) ΔS_m vs. T of three different metallic glasses ($Gd_{53}Co_{20}Al_{24}Zr_3$, $Gd_{33}Er_{22}Co_{20}Al_{25}$ and $(Er_{0.7}Ho_{0.2}Dy_{0.1})_{55}Ni_{25}Al_{20}$) under 5 kOe in bulk and stacked-ribbon forms, respectively. (d) ΔS_m vs. T of the stacked-ribbon contains three different rare-earth-based metallic glasses ($Gd_{53}Co_{20}Al_{24}Zr_3$, $Gd_{33}Er_{22}Co_{20}Al_{25}$ and $(Er_{0.7}Ho_{0.2}Dy_{0.1})_{55}Ni_{25}Al_{20}$) with the mass ratio of 1:1:1 (left-down scale), and the left-up scale shows the Gd_xDy_{1-x} composite containing five constituents with the optimum ratio (taken from ref. [10]).

ditional insight concerning the effect of the stacked-ribbon structure on the mangetocaloric response of the glassy materials. The inset of Figure 2(a) shows that the ΔT_{FWHM} of a $Gd_{53}Co_{20}Al_{24}Zr_3$ metallic glass is broader than that of pure crystalline Gd only in stacked-ribbon, but no obvious variation in the bulk form. Both the left section (ΔT_L) and right section (ΔT_R) of the ΔT_{FWHM} increase with the applied field, and ΔT_L is greatly larger than ΔT_R. Between the stacked-ribbon and bulk forms ΔT_R shows no evident change, while ΔT_L is considerably broader in the stacked-ribbon. A summary of the relative variation of ΔS_m and the refrigerant efficiency RC ($RC = \Delta S_m \cdot \Delta T_{FWHM}$) under different fields is shown in Figure 2(b). The inset shows that RC of the $Gd_{53}Co_{20}Al_{24}Zr_3$ glass is larger than that of pure crystalline Gd in a stacked-ribbon structure, but

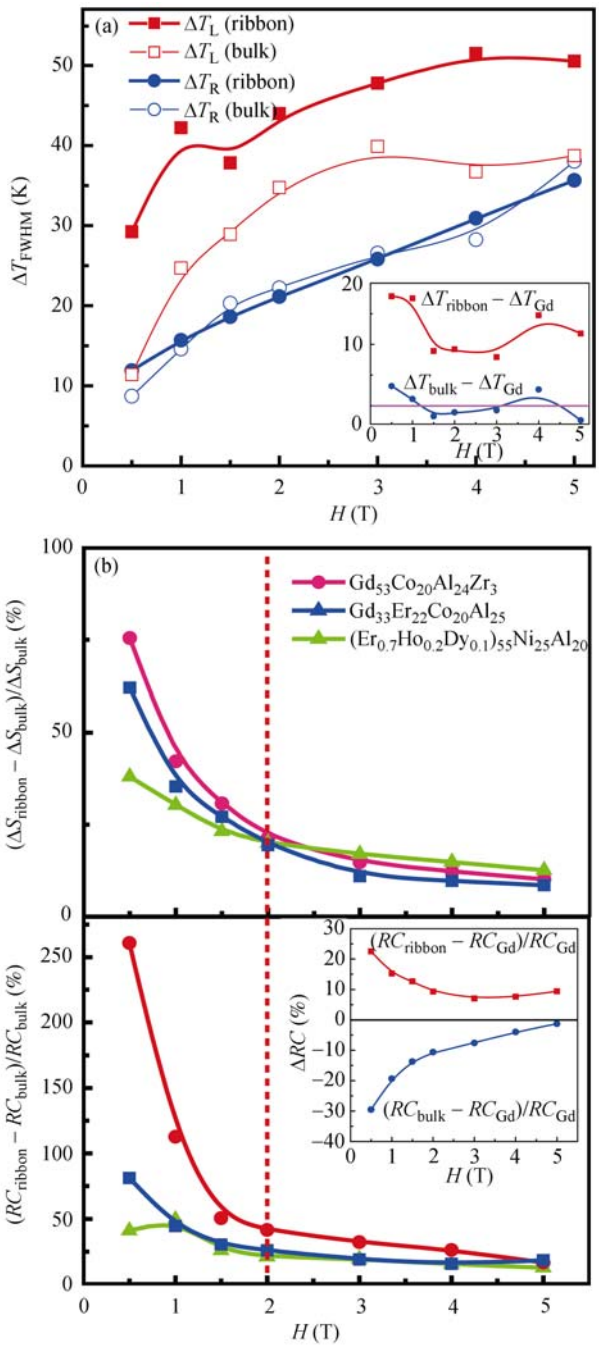

Figure 2 (a) The left section (ΔT_L) and right section (ΔT_R) of ΔT_{FWHM} variations of $Gd_{53}Co_{20}Al_{24}Zr_3$ metallic glass in bulk and stacked-ribbon forms, respectively. The inset shows the relative change of ΔT_{FWHM} of metallic glass in bulk and stacked-ribbon forms, compared with that of pure crystalline Gd. (b) The relative variation of ΔS_m and the refrigerant efficiency RC ($RC = \Delta S_m \cdot \Delta T_{FWHM}$) of different glasses ($Gd_{53}Co_{20}Al_{24}Zr_3$, $Gd_{33}Er_{22}Co_{20}Al_{25}$ and $(Er_{0.7}Ho_{0.2}Dy_{0.1})_{55}Ni_{25}Al_{20}$) under different fields. The inset shows the relative variation of RC of $Gd_{53}Co_{20}Al_{24}Zr_3$ glass in bulk and stacked-ribbon forms, compared with that of pure crystalline Gd.

smaller in the bulk form. Compared with the metallic glasses in the bulk form, ΔS_m values of various glassy stacked-ribbons have been enhanced by more than 50% at 5 kOe, and RC of some

metallic glass even increases twice. The enhancement of both ΔS_m and *RC* is more pronounced below 20 kOe, which is of great significance for practical application due to the fact that the low field (<15 kOe) can be supplied by the low-cost Nd-Fe-B permanent magnet, instead of the expensive superconductor magnet. These indicate that the stacked-ribbon structure may be a general and simple way to greatly enhance the low-field MCE of metallic glasses.

On the basis of that, further compositing progress is developed by taking advantage of the intrinsic phase separation and clustering in metallic glasses. Since $Fe_{100-x}Gd_x$ metallic glass can be made in a wide concentration range ($18 < x < 60$), its transition temperature can be tuned easily in a large temperature range[21]. The paramagnetic to ferromagnetic transition of $Fe_{100-x}Gd_x$ glassy ribbon spans over a much wider temperature region below 600 K, compared with that of the crystalline Gd. According to the Maxwell relation[2], a magnetic entropy change spreading over a wider temperature range may be expected in this glass system. However, its ferromagnetic transition is too broad and weak to be used for engineering applications. To optimize the MCE below 300 K, a FeGd-based glassy ribbon containing *in situ* formed Gd nanocrystals is obtained by taking advantage of the phase separation and clustering, which has been widely observed in the rare earth-transition metal based metallic glass, such as La-Fe, Y-Fe and Pr-Fe alloys[16]. Figure 3(a) shows the XRD patterns of the as-cast FeGd-based rods and ribbons with different wheel speeds. The broad diffraction peaks and no appreciable sharp peaks indicate that the glassy ribbons can be obtained by the higher spin velocities. When the spin velocity decreases to 10 m/s, a broadening crystalline peak is superimposed on the XRD curve due to the formation of nanocrystalline Gd, and the ribbon has a mixed microstructure of nanocrystals and glassy matrix, which is consistent with the direct atomic/magnetic force microscope (AFM/MFM) observation. In fact, the nanocrystals smaller than 2 nm, which cannot be detected within the resolution limit of the XRD, have been widely observed in Re-Fe based metallic glass by HRTEM[22,23]. The glassy nature is further confirmed by DSC measurements as shown in the inset of Figure 3(a). All alloys exhibit a sharp exothermic peak due to the massive crystallization, and no obvious endothermic event for a glass transition is visible, similar to other RE-Fe based metallic glasses[23].

Figure 3(b) shows the temperature dependence of the magnetization for FeGd-based glassy composite, pure Gd. The magnetization curves of $Fe_{100-x}Gd_x$ metallic glasses are also shown for comparison[21]. Through the well-proportioned Al doping, the ferromagnetic transition of FeGd-based glassy composite such as $Fe_{30}Gd_{60}Al_{10}$ and $Fe_{15}Gd_{70}Al_{15}$ is tuned to nearly span over the whole low-temperature range below room temperature without large saturated magnetization loss. The inset of Figure 3(b) shows that the $Fe_{30}Gd_{60}Al_{10}$ glassy composite exhibits superparamagnetic-like behavior at both 300 and 10 K, and there is nearly no magnetic hysteresis. This is a very favorable characteristic of magnetic refrigerant application, because in this case it is relatively easy to magnetize and demagnetize the material[2]. Similar superparamagnetic results were reported in the glassy ribbons of Nd(Y, Dy)FeAl alloys, in which the origin of the superparamagnetism is interpreted as the formation of ferromagnetic nanoclusters embedded in a paramagnetic glassy matrix[16,22]. It is expected that the superparamagnetic behavior of $Fe_{30}Gd_{60}Al_{10}$ glassy composite is presumably due to the existence of the ferromagnetic Gd nanocrystals with strong cluster interaction in the glassy matrix.

To confirm the ideal ferromagnetic transition of the FeGd-based glassy composite, a careful analysis of the derivative of the $M(T)$ curves with respect to temperature, dM/dT, is shown in Figure 3(c). For the $Fe_{30}Gd_{60}Al_{10}$ ribbon spun at 80 m/s, dM/dT displays a minimum at 265 K and a very

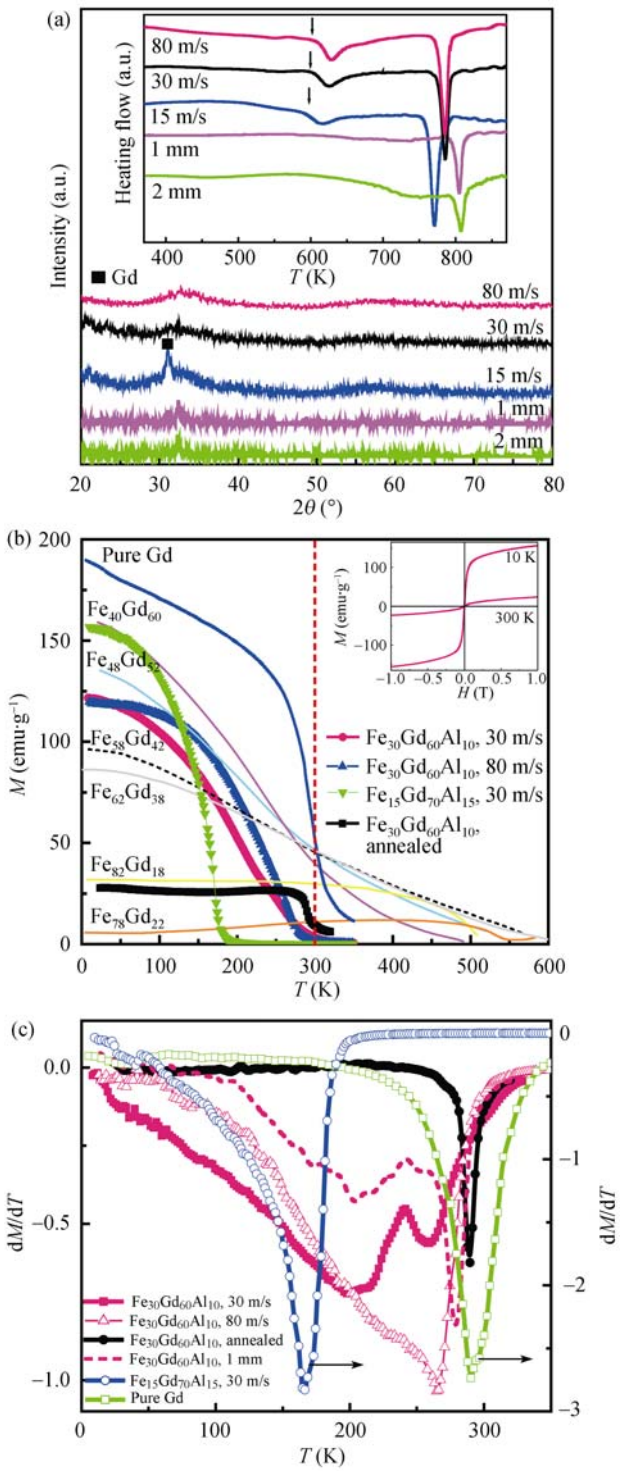

Figure 3 (a) XRD patterns of the as-quenched $Fe_{30}Gd_{60}Al_{10}$ ribbons with different wheel speeds and rods with diameters of 1—2 mm. The inset shows the DSC curves of the ribbons and rods. (b) Temperature dependence of the magnetization for $Fe_{30}Gd_{60}Al_{10}$ ribbon. The magnetization curves of $Fe_{100-x}Gd_x$ glassy ribbons (taken from ref. [21]), pure Gd, and $Fe_{30}Gd_{60}Al_{10}$ annealed alloy are shown for comparison. The inset shows the magnetization loops of $Fe_{30}Gd_{60}Al_{10}$ ribbon at 300 and 10 K. (c) The derivative dM/dT of $Fe_{30}Gd_{60}Al_{10}$ ribbon (left scale), $Fe_{15}Gd_{70}Al_{15}$ ribbon (right scale) and pure Gd (right scale).

broad shoulder around 230 K. When the wheel speed decreases to 30 m/s, dM/dT shows two successive pronounced minima around 260 and 200 K. For a 1 mm rod, there also exist two minima around 280 and 200 K. Considering that the bulk Gd polycrystalline has a Curie temperature of 294 K, the minima at the higher temperature shall be attributed to the ferromagnetic transition of the *in situ* formed Gd nanocrystals, and the lower one originates from glassy matrix. Here we mark the higher transition temperature as T_{nano} and the lower as T_{amor}. It is interesting that dM/dT at T_{nano} and T_{amor} are more comparable in the appropriate compositions and cooling rates: For $Fe_{15}Gd_{70}Al_{15}$ ribbon with a lower Fe content, the glass forming ability is enhanced so that dM/dT at T_{amor} is dominant; while for a lower cooling rate (1 mm $Fe_{30}Gd_{60}Al_{10}$ rod), the nanocrystals with more volume fraction are retained in the matrix and dM/dT at T_{nano} is pronounced. Therefore, by virtue of the easily-tuned cooling rate and compositions, the suitable fraction between the nanocrystals and glassy matrix plays a crucial role for the two successive and comparable ferromagnetic transitions in the FeGd-based glassy composite. In addition, both the transition range and the saturated magnetization of the corresponding annealed alloy with fully crystallized state decrease sharply, further confirming that the nature of the glassy matrix composite is the key point of the multiple broad magnetic transitions and large saturated magnetization.

The isothermal magnetization curves (M-H) of FeGdAl glassy composite with increasing field in a wide temperature range are shown in Figure 4(a) and (b). By computing from the isothermal M-H curves, the variation of ΔS_m, as a function of temperature under 50 kOe, is shown in Figure 4(c). For comparison, the magnetocaloric properties of other representative materials are listed in Table 1 and Figure 4(d). ΔS_m of the $Fe_{30}Gd_{60}Al_{10}$ composite is about 3.53 $J \cdot kg^{-1} \cdot K^{-1}$, which is half of the well-known crystalline magnetic refrigerant compound $Gd_5Si_2Ge_{1.9}Fe_{0.1}$[2], but the ΔS_m peak is so broad that the FWHM (from 303 to 30 K) nearly spreads over the whole low temperature range, which is five times wider than that of $Gd_5Si_2Ge_{1.9}Fe_{0.1}$ and pure Gd, even ten times wider than that of $Gd_5Si_2Ge_2$ and $MnFeP_{0.45}As_{0.55}$[3,4]. ΔS_m of the annealed composite slightly increases to 5 $J \cdot kg^{-1} \cdot K^{-1}$, similar to the other FeGd-based crystal alloys[24]. However, the FWHM decreases sharply to 20 K, which is only one fourteenth of that of the glassy sample, confirming that the glassy structure plays a dominant role in the broadened FWHM. Interestingly, for the FeGd-based glassy composite spun at 30 m/s, the maximum ΔS_m approaches a nearly constant value in a wide temperature span over 100 K (from 120 to 220 K), and when increasing the wheel velocity to 80 m/s the table-like region is shifted between 160 and 260 K. Two important features can be found from this region. One is that the table-like region around ΔS_m ~3.5 $J \cdot kg^{-1} \cdot K^{-1}$ compares favorably with that in the complex multi-component composite system such as La(FeCo)Al composite (~2.5 $J \cdot kg^{-1} \cdot K^{-1}$)[7], DyAl-based composite (~4 $J \cdot kg^{-1} \cdot K^{-1}$)[6], and GdDy-based composite (~5 $J \cdot kg^{-1} \cdot K^{-1}$)[10]. Although a composite system consists of different compounds that individually have high ΔS_m, ΔS_m for the composite is usually small due to different lattice entropy contributions of each component in the selected temperature range[7]. Another feature is that the table-like region is much broader and smoother than that of conventional composites with more constituents, where the different magnitude peaks in $\Delta S_m - T$ curves are widely observed. The broad table-like ΔS_m region makes FeGd-based glassy composite attractive for applications in the Ericsson magnetic cycle below room temperature. In addition, the MCE material such as GGG ($Gd_3Ca_5O_{12}$) has been

Table 1 Magnetic entropy changes and related parameters of different alloys under 50 kOe[a)]

Material	Structure	ΔS_m ($J \cdot kg^{-1} \cdot K^{-1}$)	Transition temperature (K)	ΔT_{FWHM} (K)	RC ($J \cdot K^{-1}$)			Ref.
					RC_1	RC_2	RC_3	
$Fe_{30}Gd_{60}Al_{10}$	a + c	3.53	200	273	964	754	488	Present work
$Fe_{15}Gd_{70}Al_{15}$	a + c	6.12	170	169	1034	764	500	Present work
$Gd_{33}Er_{22}Al_{25}Co_{20}$	a	9.47	52	75	714	574	359	Present work
$Gd_{53}Al_{24}Co_{20}Zr_3$	a	9.4	93	83	780	590	375	Present work
Gd	c	9.43	294	71	670	514	338	–
$Gd_5Si_2Ge_{1.9}Fe_{0.1}$	c	7	276	51	357	360	240	[2]
$MnFeP_{0.45}As_{0.55}$	c	18.3	306	21	390	341	229	[3]
$Gd_5Si_2Ge_2$	c	18.6	276	16	298	305	265	[4]
$Pd_{40}Ni_{22.5}Fe_{17.5}P_{20}$	a	0.58	94	–	–	–	–	[18]
$Fe_{33}Gd_{27}Al_{40}$	c	4.67	174	87	406	320	194	[24]
DyNiAl	c	19	256	33	627	483	312	[25]
$(Fe_{85}Co_5Cr_{10})_{91}Zr_7B_2$	a	2.8	320	167	468	360	240	[26]
$Fe_{57}Cr_{17}Cu_1Nb_3Si_{13}B_9$	a	0.86	150	150	129	109	67	[27]
La $(Fe_{0.89}Si_{0.11})_{13}$	c	24	188	9	216	190	148	[28]
$La_{0.7}Ca_{0.3}MnO_3$	c	6.4	228	36	230	185	116	[29]
$Ni_2Mn_{0.75}Cu_{0.25}Ga$	c	65	308	2	72	130	51	[30]

a) a and c stand for the amorphous and crystalline states, respectively.

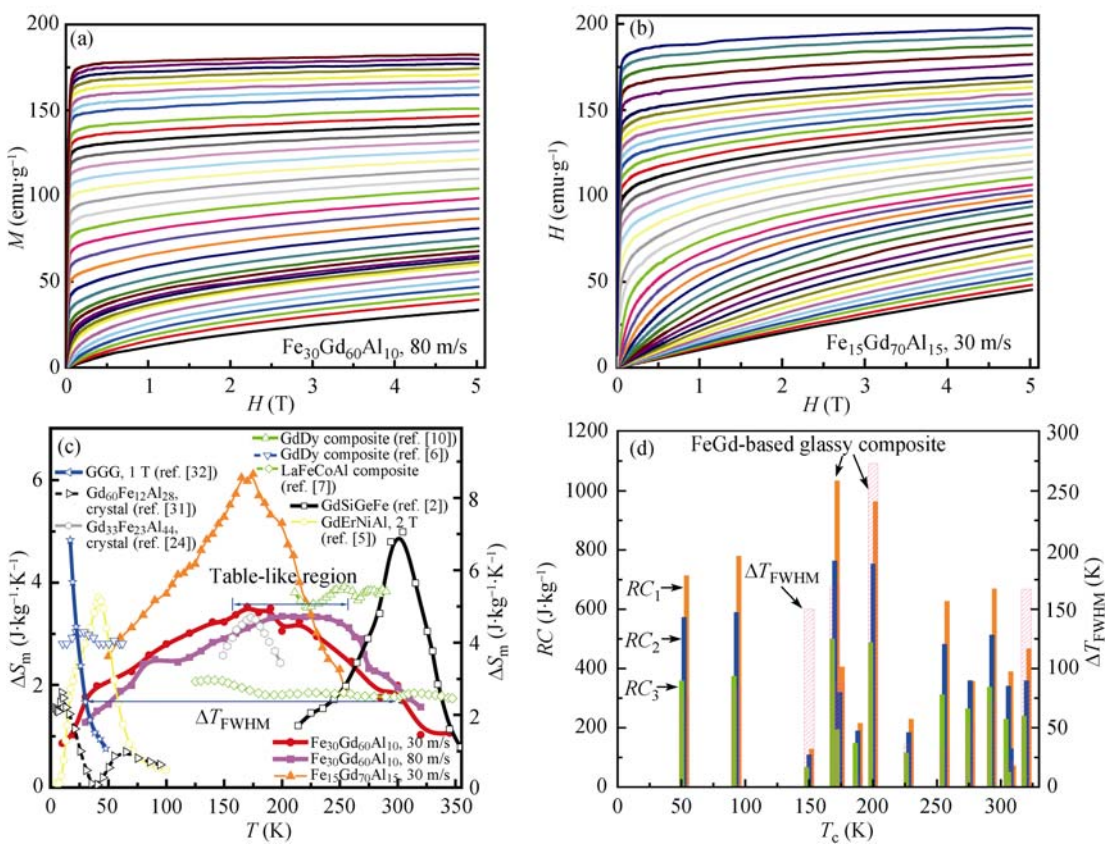

Figure 4 (a) Isothermal magnetization vs. field curves for the $Fe_{30}Gd_{60}Al_{10}$ ribbon spun at 80 m/s between 10 and 350 K; (b) isothermal magnetization vs. field curves for the $Fe_{15}Gd_{70}Al_{15}$ ribbon spun at 30 m/s between 50 and 260 K; (c) ΔS_m vs. T for the FeGd-based ribbon under 50 kOe (left scale), and the ΔS_m curves of other representative magnetocaloric materials are shown for comparison (right scale); (d) the refrigerant capacity (RC_1, RC_2, RC_3) calculated by three different methods (left scale) and ΔT_{FWHM} as a function of a Curie temperature in a field change of 50 kOe (right scale).

widely used in the commercial magnetic refrigerant application below 15 K[32], and therefore, the current FeGdAl glassy composite may be a good candidate to cooperate with GGG materials as a teamwork for a continuous magnetic refrigeration from room temperature to a very low temperature, which covers all of the important nitrogen, hydrogen and helium liquefaction temperature ranges.

In general, the best MCE materials supply the maximum amount of cooling over the widest temperature range[5]. A compromise between the magnitude of the magnetic entropy change and the width of the peak is necessary for a working prototype, giving rise to the refrigerant capacity as a suitable metrics for comparing the performance of different materials. The *RC* values can be measured in literature by three main methods, and have been widely used as a very important parameter characterizing the materials' refrigerant efficiency[2,15]: (a) The product of the peak entropy changes times the FWHM of the peak, $RC_1 = \Delta S_m \cdot \Delta T_{FWHM}$; (b) by numerically integrating the area under the $\Delta S_m(T)$ curves, and using the temperature at half maximum of the peak as the integration limit, $RC_2 = \Delta S_{area}$; (c) defining *RC* of a reversible refrigeration cycle operating between T_h and T_c (the temperature of the hot and cold reservoirs, respectively) as $RC_3 = \Delta S_m \cdot \Delta T$, where ΔS_m is the magnetic entropy change at the hot and cold ends of the cycle and $\Delta T = T_h - T_c$. No matter which method is chosen as a criterion, the obtained *RC* value of the FeGd-based glassy composite is remarkably larger than that of other typical magnetic refrigerants (see Figure 4(d)). For example, the $RC_1 = \Delta S_m \cdot \Delta T_{FWHM}$ values for $Fe_{30}Gd_{60}Al_{10}$ and $Fe_{15}Gd_{70}Al_{15}$ glassy composites are determined to be 964 $J \cdot kg^{-1}$ and 1034 $J \cdot kg^{-1}$, which are more than double the *RC* of the well-known refrigerant compound $Gd_5Si_2Ge_{1.9}Fe_{0.1}$ (357 $J \cdot kg^{-1}$) and $MnFeP_{0.45}As_{0.55}$ (390 $J \cdot kg^{-1}$). The optimal refrigeration cycle maximizes both *RC* and ΔT_{FWHM}, which is perfectly implemented in the FeGd-based glassy composite. It is noted that the total area below the ΔS_m vs. *T* curve for the high Fe content glassy composite is roughly similar to that with the low Fe content, i.e. the similar *RC* value. Therefore, the content of Fe not only tunes the ferromagnetic to paramagnetic transition temperature, but also allows selecting the abrupt or gradual ΔS_m change around the transition temperature without large *RC* loss.

4 Discussion

The giant enhancement of MCE in FeGd-based alloy should be ascribed to the microstructure of the glassy composite, which leads to the coexistence of the broad table-like region, the large *RC* and ΔT_{FWHM}. Firstly, the glassy nature plays a dominating role in achieving the enhanced MCE, which changes the abrupt paramagnetic-ferromagnetic transition in crystal alloys to gradual implementation, greatly broadening the transition temperature range with large magnetic moments retained. The FeGd-based glassy composite is selected owing to the Gd having much larger magnetic moment and relatively small magnetocrystalline anisotropy for the absent orbit momentum[15]. Secondly, the more uniformly oriented magnetic microstructure and homogenous element distribution resulting from the high cooling rate by melt spinning[33] induce more activated and grouped ferromagnetic moments below Curie temperature in the stacked glassy composite ribbon, which are easier to adjust and preferentially realign along the applied magnetic field than the independent ones in bulk materials[34]. Easier alignment of magnetic spins not only gives rise to larger ΔS_m even in the low field, but also broadens the ΔS_m peak greatly. Finally, considering Gd with a Curie temperature very close to room temperature (294 K), the FeGd-based stacked-ribbons

with each ribbon composed of glassy matrix and *in situ* formed Gd nanocrystals have the multiple successive ferromagnetic transitions, which engenders that the maximum ΔS_m approaches a nearly constant value in a wide temperature span over 100 K, and the ΔT_{FWHM} almost spans over the whole low-temperature range below room temperature. In essence, the table-like ΔS_m and broad ΔT_{FWHM} may result from the highly inhomogeneous ferromagnetic exchange interaction that is expected to arise from the random neighbors (Fe and Al) of Gd magnetic moments. Compared to a simple ferromagnet, a highly inhomogeneous ferromagnet, such as FeGd-based glassy composite, has a spatially inhomogeneous distribution of a local Curie temperature so that the heat capacity and corresponding magnetic entropy change peak are greatly broadened[35]. Moreover, by grouping spins together in superparamagnetic clusters, the magnetic moments are more easily aligned in a broader temperature range and lower magnetic field. Similar type of magnetic nanocomposite morphology also has dramatic effect on the MCE in $Gd_5Ge_2Si_2$ and $Gd_3Ga_5O_{12}$ crystals by Fe doping[2,32].

5 Conclusions

The FeGdAl metallic glass composite with the broad table-like region over 100 K, large *RC* up to 10^3 J·kg^{-1}and large ΔT_{FWHM} ranging from 303 to 30 K opens up the possibility of using this system for the efficient Ericson-cycle magnetic refrigeration. The partial substitution of Gd and replacement of the expensive and poisonous elements using low-cost Fe and Al can greatly reduce the cost of refrigerant alloys (e.g. the price of Fe is only a few percents of Gd), and the glassy ribbon composite is very compatible with large-scale production technologies. The structure and composition of the FeGdAl metallic glass matrix composite can be easily tuned by controlling Fe content and the cooling rate, and the ΔS_m value of the materials could be further enhanced to satisfy the commercial engineering applications by the appropriate composition choice and processing control.

1 Krenke T, Duman E, Acet M, et al. Inverse magnetocaloric effect in ferromagnetic Ni-Mn-Sn alloys. Nat Mater, 2005, 4: 450－454[DOI]

2 Provenzano V, Shapiro A J, Shull R D. Reduction of hysteresis losses in the magnetic refrigerant $Gd_5Ge_2Si_2$ by the addition of iron. Nature, 2004, 429: 853－857[DOI]

3 Tegus O, Bruck E, Buschow K, et al. Transition-metal-based magnetic refrigerants for room-temperature applications. Nature, 2002, 415: 150－152[DOI]

4 Pecharsky V K, Gscheidner K A Jr. The giant magnetocaloric effect in $Gd_5(Ge_2Si_2)$. Phys Rev Lett, 1997, 78: 4494－4497 [DOI]

5 Korte B J, Pecharsky V K, Gschneidner K A Jr. The correlation of the magnetic properties and the magnetocaloric effect in $(Gd_{1-x}Er_x)$NiAl alloys. J Appl Phys, 1998, 84: 5677－5685[DOI]

6 Hashimoto T, Kuzuhara T, Matsumoto K, et al. A new method of producing the magnetic refrigerant suitable for the Ericsson magnetic refrigeration. IEEE Trans Mag, 1987, 23: 2847－2849[DOI]

7 Gomesa A M, Proveti J R, Takeuchi A Y, et al. $La(Fe_{1-x}Co_x)_{11.44}Al_{1.56}$: A composite system for Ericsson-cycle-based magnetic refrigerators. J Appl Phys, 2006, 99: 116107[DOI]

8 Luo Q, Zhao D Q, Pan M X, et al. Magnetocaloric effect of Ho-, Dy-, and Er-based bulk metallic glasses in helium and hydrogen liquefaction temperature range. Appl Phys Lett, 2007, 90: 211903[DOI]

9 Hashimoto T, Kuzuhura T, Sahashi M, et al. New application of complex magnetic materials to the magnetic refrigerant in an Ericsson magnetic refrigerator. J Appl Phys, 1987, 62: 3873－3878[DOI]

10 Smaili A, Chahine R. Composite materials for Ericsson-like magnetic refrigeration cycle. J Appl Phys, 1997, 81: 824 －829 [DOI]

11 Shao Y Z, Zhang J X, et al. Magnetic entropy in nanocomposite binary gadolinium alloys. J Appl Phys, 1996, 80: 76－80 [DOI]
12 Wang D H, Han Z D, Huang S L, et al. The low-field magnetic entropy change in melt-spun and annealed Gd ribbons. Physica B, 2004, 352: 185－189[DOI]
13 Hou X L. Research on magnetocaloric effect of GdAl alloy. Rare Metal Mater Engin, 2006, 35: 749－751
14 Zhang T B. The structure and magnetocaloric effect of rapidly quenched $Gd_5Si_2Ge_2$ alloy with low-purity gadolinium. Mater Lett, 2007, 61: 440－443[DOI]
15 Luo Q, Zhao D Q, Pan M X, et al. Magnetocalroric effect in Gd-based bulk metallic glass. Appl Phys Lett, 2006, 89: 081914 [DOI]
16 Kong H Z, Ding J, Dong Z J, et al. Observation of clusters in $Re_{60}Fe_{30}Al_{10}$ alloys and the associated magnetic properties. J Phys D, 2002, 35: 423－429[DOI]
17 Wang W H. Correlations between elastic moduli and propertyes in bulk metallic glasses. J Appl Phys, 2006, 99: 093506 [DOI]
18 Shen T D, Schwarz R B, Coulter J Y, et al. Magnetocaloric effect in bulk amorphous $Pd_{40}Ni_{22.5}Fe_{17.5}P_{20}$ alloy. J Appl Phys, 2002, 91: 5240－5245 [DOI]
19 Yavari A R. The changing faces of disorder. Nat Mater, 2007, 6: 181－182[DOI]
20 Greer A L. Metallic glasses. Science, 1995, 267: 1947－1953[DOI]
21 Yano K, Akiyama Y, Tokumitsu K, et al. Magnetic moment and Curie temperature for amorphous $Fe_{100-x}Gd_x$ alloys. J Mag Mag Mater, 2000, 214: 217－224[DOI]
22 Chen D, Takeuchi A, Inoue A. Thermal stability and magnetic properties of Gd-Fe-Al bulk amorphous alloys. J Alloys Comp, 2007, 440: 199－203[DOI]
23 Yoshiike S, Adachi H, Ichinose H, et al. Structure of melt-quenched Pr-Fe alloys and analysis of the magnetization based on super-ferromagnetism. JIM, 1998, 39: 102－109
24 Xiong D K, Li D, Liu W, et al. Magnetocaloric effect of $Gd(Fe_xAl_{1-x})_2$ compounds. Physica B, 2005, 369: 273－277[DOI]
25 Singh N K, Suresh K G, Nirmala R, et al. Correlation between magnetism and magnetocaloric effect in the intermetallic compound DyNiAl. J Appl Phys, 2006, 99: 08K904[DOI]
26 Johnson F, Shull R D. Amorphous FeCoCrZrB ferromagnets for use as high-temperature magnetic refrigerants. J Appl Phys, 2006, 99: 08K909[DOI]
27 Kolat V S, Atalay S. Magnetocaloric behavior in $Fe_{57}Cr_{17}Cu_1Nb_3Si_{13}B_9$ soft magnetic alloys. Phys Stat Sol, 2004, 1: 3529－3532[DOI]
28 Fujieda S, Fujita A, Fukamichi K. Large magnetocaloric effect in $La(Fe_xSi_{1-x})_{13}$ itinerant-electron metamagnetic compounds. Appl Phys Lett, 2002, 81: 1276－1278[DOI]
29 Phan M H, Yu S C. Review of the magnetocaloric effect in manganite materials. J Mag Mag Mater, 2007, 308: 325－340 [DOI]
30 Stadler S, Khan M, Mitchell J, et al. Magnetocaloric properties of $Ni_2Mn_{1-x}Cu_xGa$. Appl Phys Lett, 2006, 88: 192511[DOI]
31 Provenzano V, Shapiro A J, Shull R D, et al. Peak magnetocaloric effects in Al-Gd-Fe alloys. J Appl Phys, 2004, 95: 6909－6911[DOI]
32 McMichael R D, Ritter J J, Shull R D. Enhanced magnetocaloric effect in $Gd_3Ga_{5-x}Fe_xO_{12}$. J Appl Phys, 1993, 73: 6946－6948[DOI]
33 Yan A, Müller K H, Schultz L, et al. Magnetic entropy change in melt-spun MnFePGe. J Appl Phys, 2006, 99: 08K903 [DOI]
34 McMichael R D, Shull R D, Swartzendurber L J, et al. Magnetocaloric effect in superparamagnets. J Mag Mag Mater, 1992, 111: 29－33[DOI]
35 Nirmala R, Morozkin A V, Malik S K, et al. Magnetocaloric effect in the intermetallic compound $Gd_5Si_2Sb_2$. Europhys Lett, 2005, 72: 652－657[DOI]